Journal of Solar Energy Research (JSER)

Journal homepage: jser.ut.ac.ir

Thermoeconomic Analysis of an Ammonia-water mixture CCHP Cycle with Solar Collectors

A. Hajizadeh Aghdam [a,*], M. Borzabadi Farahani [b], A. Davodabadi Farahani[c],

[a,b,c] *Department of Mechnical Engineering, Arak University of Technology, Arak 38181-41167, Iran*

Received: 2020-05-30
Accepted: 2020-08-26

A B S T R A C T

In this paper, a system of simultaneous production of power and heat and cooling in a Kalina cycle has been analyzed by energy, exergy and economic aspects. To provide heat in the cycle heating unit, four types of solar thermal linear (PTC) and linear share (LFR) heat collectors, plate (dish) and vacuum tube, have been used. The results of the analysis of this cycle for the PTC collector compared to other collectors showed that this collector was superior in increasing the energy and exergy efficiencies of the system and also lowering the total cost rate and exergy destruction of the CCHP cycle. By using parametric studies tried to obtain the effect of increasing and decreasing some of the cycle component parameters to get the most cooling, heating and power output.

Keywords: Thermoeconomic; Kalina cycle; Solar heater

1. Introduction

Over the past decades, scientist and engineers have tried various ways to develop high-efficient integrated energy systems to directly transfer low-grade heat sources (e.g., solar energy, wind energy, solar pond, geothermal energy, etc.) to electricity, space heating, and cooling. Among them, combined cooling, heating, and power (CCHP) systems are known as energy system distributors and provide following benefits: simultaneous electricity, heating, and cooling production with high efficiency, significant reduction in greenhouse gas emissions, fuel and energy demand with low costs and other benefits. Numerous studies considered economic and thermal efficiency criteria into the design of CCHP systems with solar collectors, For example: Chen et al.[1] discussed on the off-design behavior of a CCHP cycle based on the GT cycle and proved that this system saves energy as the gas turbine power exceeds 30% of the total load. Colin et al. [2] Examined a 3 MW solar-powered Rankin organic cycle for a region in South Africa .The system used ۷۰m۲ area linear share collector with solar tracking as well as a by volume $2m^3$ quartz heat storage source to store solar energy. Manalacus et al. Designed a simultaneous power generation and water desalination system based on the solar cell cycle [3]. in The system uses vacuum tube collectors with a solar energy level of 216 m^2. Wang et al. Examined a solar ORC system with a production capacity of 1.73 kW [4]. In this system, which used flat panel collectors and vacuum tube collectors in parallel, solar energy was used directly to increase the operating fluid temperature of the ORC cycle. Wang et al. Examined a low-temperature reheating ORC system. In this study, a flat plate collector has been used because it has a low cost [5]. The heat storage source is also used to continuously generate power. Lee et al. Investigated a solar ORC system with a linear contribution collector with R-123 operating fluid [6]. In the storage source used in this system, phase change materials have been used, which leads to continuous power generation. Wang et al. Examined the performance of the solar cycle at low temperatures using several ze otropic mixtures [6]. The

*A.Hajizadeh@arakut.ac.ir

results showed that the use of these materials, in addition to expanding the scope of choice of the operating fluid, also increases the thermal efficiency of the system. They also experimentally compared the effects of pure fluids and zeotropic mixtures for system performance, and concluded that the zeotropic mixture increased the overall efficiency of the ORC system. Suleiman et al. Compared the performance of a simultaneous power generation system with heat and cold in three modes [7,8]. In the first case, it used solar energy and linear share collectors, in the second case, it used fuel cells, and in the third case, it used geothermal energy to set up the system. The system is optimized for the use of solar energy from a thermodynamic point of view, and the energy efficiency and exergy of the system in this mode are 94% and 18%, respectively. Carlas developed a triple production system of power and heating and cooling based on the Organic Rankin cycle, thermodynamic modeling and economic analysis [9]. In this system, a compression refrigeration cycle is used for cooling. Two sources of solar energy and biomass have been used to power the system.

Therefore, in this study, a new ammonia-water mixture CCHP driven by a low-grade heat source is proposed which is basically a modified version of the Kalina cycle (KC). In this research, thermodynamic analysis from the perspective of: energy, exergy and economics for a solar system with four different types of collectors in different conditions has been done. The task of this system is to meet the needs of electricity, heating and cooling based on a Kalina cycle.

1. Materials and Methods

2.1. Thermodynamic modelling

CCHP systems provide technologies development towards more sustainable energy systems, particularly when renewable energies are used as heat source. solar energy is currently believed to be one of the most advantageous sources of energy for trigeneration purposes. Not only is it a renewable type of energy but also present in most areas.

Schematic diagram of the recommended ammonia-water CCHP system is displayed in Fig 1.

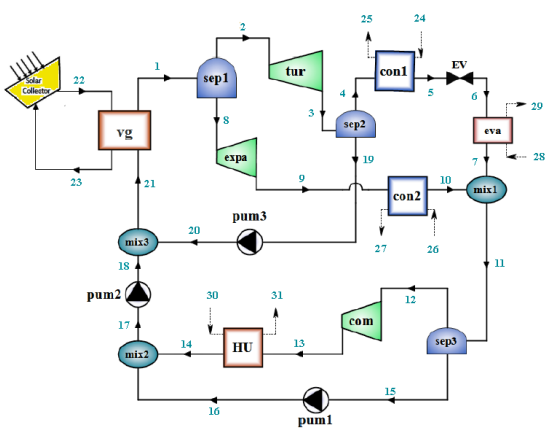

Figure 1. Ammonia-water CCHP system

This system is run by a LTHS (solar energy) and is based on the KC consisting of two turbines, a vapor generator, three separators, an expansion valve, three mixers, two condensers, an evaporator, a heating unit (HU) system, a compressor, and three pumps.

Upon gaining some specific energy from the LTHS (state 22), the two-phase mixture at the outlet of vapor generator (state 1) is separated into the rich saturated vapor (state 2) and poor saturated liquid (state 8). The saturated vapor goes through turbine 1 and expands to a condensation pressure to generate electricity from turbine 1, and then enters separator 2 (state 3), that is then separated into two richer (state 4) and leaner (state 19) streams. The richer flow enters the condenser 1 (state 5) which is cooled by external water circulation and then throttled to the low pressure of evaporator by an expansion device (state 6). This two-phase flow is then heated up to evaporation temperature by outlet water and enters a mixer, while producing cooling capacity for cooling users (state 7). Meanwhile, the lean saturated liquid (state 8) is throttled to the low pressure of condenser 2 by expander (state 9) to produce expander output power, which is cooled down in condenser 2 and entered the mixer 1 (state 10). The evaporator outlet saturated vapor is mixed with the condenser 2 outlet saturated liquid in the mixer 1 and the mixed flow goes through the separator 3 (state 11). This two-phase flow is separated into saturated vapor (state 12) and liquid (state 15), where the saturated vapor is compressed to the heating unit pressure by compressor (state 13) and then enters the HU system to produce heating output for heating users (state 31) and then enters the mixer 2 (state 14). The saturated liquid mixture (state 15) is pumped to higher pressure of the HU system by pump 1 (state 16) and then mixed with HU outlet stream. The mixed flow (state 17) is boosted to higher pressure of vapor generator and then enters the mixer 3 (state 18). Meanwhile, the leaner ammonia-water saturated liquid (state 19) is boosted to the high pressure of vapor generator by pump 3 and then mixed with pump 2 outlet flow in mixer 3 (state 20). The mixed flow then fed into the vapor generator (state 21), completing the proposed CCHP system process.

2. Thermodynamic analysis

Employing general mass, concentration, and energy conservative equations into account for each component, then:

Mass balance equation:

$$\sum_i \dot{m}_{in} = \sum_o \dot{m}_{out} \quad (1)$$

Concentration balance equation:

$$\sum(\dot{m}X)_{in} = \sum(\dot{m}X)_{out} \quad (2)$$

where, X is the mass concentration of NH3 in the solution.

Energy balance equation:

$$\dot{Q}_{c.v.} - \dot{W}_{c.v.} = \sum(\dot{m}h)_{out} - \sum(\dot{m}h)_{in} \quad (3)$$

The exergy-based balance equation for kth component of the system may be written as:

$$\dot{I}_{D,k} = \sum_{i=1}^{k} \psi_{in,i} - \sum_{i=1}^{k} \psi_{out,i} \quad (4)$$

Due to the small values of the kinetic and potential exergies, their values are not accounted on the overall exergy, and hence:

$$\psi_k = \psi_{ph,k} + \psi_{ch,k} \quad (5)$$

Where:

$$\psi_{ph,k} = \dot{m}(h - h_0 - T_0(s - s_0))_k \quad (6)$$

$$\psi_{ch,k} = \dot{m}\left(\left[\frac{ex^0_{ch,NH_3}}{M_{NH_3}}\right]X + \left[\frac{ex^0_{ch,H_2O}}{M_{H_2O}}\right](1-X)\right)_k \quad (7)$$

in which, 0 refers to the environment condition. Also, $ex^0_{ch,i}$ is the standard chemical exergy.

The exergy efficiency of a system may be defined as:

$$\eta_{ex,k} = \frac{Exergy\ of\ product}{Total\ supplied\ exergy} = \frac{\psi_{out}}{\psi_{in}} = \frac{\dot{I}_{P,k}}{\dot{I}_{F,k}} \quad (8)$$

3. Thermoeconomic analysis

Cost-based balance equation and auxiliary equations are employed throughout thermoeconomic analysis for every component of the system. The balance equation for cost analysis in the kth component of a cycle may be expressed as:

$$\dot{C}_{q,k} + \sum \dot{C}_{in,k} + \dot{Z}_k = \dot{C}_{w,k} + \sum \dot{C}_{out,k} \quad (9)$$

where:

$$\dot{C}_{in,k} = c_{in,k}\psi_{in,k}, \dot{C}_{out,k} = c_{out,k}\psi_{out,k}$$
$$\dot{C}_{w,k} = c_{w,k}\psi_{w,k}, \dot{C}_{q,k} = c_{q,k}\psi_{q,k} \quad (10)$$

The overall cost rate associated with the kth component may attain by:

$$\dot{Z}_k = CRF * \frac{\varphi_r * 365 * 24}{N} * Z_k \quad (11)$$

The above equation, N is the annual number of operation hours for the unit (N = 7000 hr), φ_r is the maintenance factor (φ_r = 1.06), Z_k is the purchase cost of the kth component which is listed in the Table 1 for each component, and CRF stands for the capital recovery factor, where its definition is given in the following form:

$$CRF = \frac{k(1+k)^{n_r}}{(1+k)^{n_r}-1} \quad (12)$$

Here, k denotes the interest rate (k = 0.15) and n_r is the total operating period of the system in years (n_r = 20 yr).

The exergy destruction cost of the kth component may express as below:

$$\dot{C}_{D,k} = c_F \psi_{D,k} \quad (13)$$

The relative cost difference (r_k) and exergeoeconomic factor (f_k) for the kth component of a system may be expressed respectively as:

$$r_k = \frac{(c_{P,k} - c_{F,k})}{c_{F,k}} \quad (14)$$

$$f_k = \frac{\dot{Z}_k}{(\dot{Z}_k + \dot{C}_{D,k})} \quad (15)$$

Table 1.Purchase cost equations for components

Component	Purchase cost equation
Condenser 1	$Z_{con1} = 130\left(\frac{A_{con}}{0.093}\right)^{0.78}$
Condenser 2	$Z_{con2} = 130\left(\frac{A_{con}}{0.093}\right)^{0.78}$
Turbine	$Z_{tur} = 4405\left(\dot{W}_{tur}\right)^{0.7}$
Expander	$Z_{expa} = 4405\left(\dot{W}_{expa}\right)^{0.7}$
Evaporator	$Z_{eva} = 130\left(\frac{A_{eva}}{0.093}\right)^{0.78}$
Pump	$Z_{pum} = 2100\left(\frac{\dot{W}_{pum}}{10}\right)^{0.26}\left(\frac{1-\eta_{is,pum}}{\eta_{is,pum}}\right)^{0.5}$
Vapor generator	$Z_{vg} = 130\left(\frac{A_{vg}}{0.093}\right)^{0.78}$
Heating Unit	$Z_{HU} = 130\left(\frac{A_{HU}}{0.093}\right)^{0.78}$
Solar collector	$Z_{col} = 567A_{col}$
Compressor	$Z_{eva} = 9624.2\dot{W}_{comp}^{0.46}$

Based on the definition of logarithmic mean temperature difference (ΔT_{LMTD}) and the overall heat transfer coefficient (U_k), the heat transfer value may be computed as:

$$\dot{Q}_k = U_k A_k LMTD_k \quad (16)$$

The overall heat transfer coefficient for each heat exchangers is listed in Table 2.

Table 2. The overall heat transfer coefficient for heat exchangers

Component	U(kW/m^2.k)
Vapor generator	1.6
Heating Unit	1
Condenser	1.1
Evaperator	0.9

4. Solar collectors

In this study, four types of solar collectors were used, which are vacuum tube, thermal linear (PTC), Linear share(LFR) and Plate(Dish) collectors, respectively. Using the following equation, the collector efficiency is calculated.

$$\eta_{col} = c_0 - c_1 \frac{T_{ave}-T_0}{G_{tot}} - c_2 \frac{(T_{ave}-T_0)^2}{G_{tot}} \quad (17)$$

Where the fixed coefficient of the collector test in the Table 3 for each collector is reported.[10].

Table 3. The fixed coefficient of the collector test

collector	c_0	c_1	c_2
Vacuum tube	0.612	0.54	0.0017
PTC	0.74	0.00432	0.000503
LFR	0.65	0.1	0
Dish	0.65	0.35	0.00002

G_{tot} is also the sum of scattered and direct radiation on the sloping surface of the collector.

On the other hand, efficiency is obtained from the following equation:

$$\eta_{col} = \frac{\dot{Q}_{col}}{G_{tot} A_{col}} \quad (18)$$

$\dot{Q}_{col}$ is the rate of heat transfer in the collector and A_{col} the area required by the solar collector.

5. Output parameters

The energy efficiency of the recommended ammonia-water mixture CCHP system may be stated in terms of input heat ($G_{tot}.A_{col}$), cooling capacity ($\dot{Q}_{eva}$), heating capacity ($\dot{Q}_{HU}$), net produced power ($\dot{W}_{net}$) as follows:

$$\eta_{en} = \frac{\dot{W}_{net}+\dot{Q}_{HU}+\dot{Q}_{eva}}{G_{tot}.A_{col}} \quad (19)$$

$$\dot{W}_{net} = \dot{W}_{tur} + \dot{W}_{expa} - \dot{W}_{comp} - \dot{W}_{pum1} - \dot{W}_{pum2} - \dot{W}_{pum3} \quad (20)$$

The exergy efficiency of the recommended ammonia-water mixture CCHP system expressed as below:

$$\eta_{ex} = \frac{\dot{W}_{net}+(\psi_{29}-\psi_{28})+(\psi_{31}-\psi_{30})}{\dot{E}x_{col}} \quad (21)$$

Where:

$$\dot{E}x_{col} = A_{col} * G_{tot} * \left(1 - \frac{T_0}{T_{sun}}\right) \quad (22)$$

That T_{sun} is considered equal to 4500 kelvin.

where, $\dot{C}_{W,net}$ is the net electricity cost rate of the ammonia-water mixture CCHP system and is defined as:

$$\dot{C}_{net} = \dot{C}_{tur} + \dot{C}_{expa} - \dot{C}_{comp} - \dot{C}_{pum1} - \dot{C}_{pum2} - \dot{C}_{pum3} \quad (23)$$

Also, the overall cost rate for the cchp cycle is obtained from the relation (24):

$$\dot{C}_{tot} = \sum \dot{Z}_k + \sum \dot{C}_{D,k} \quad (24)$$

6. Results and discussion

All equations of mass and energy conservation, as well as the relations related to energy analysis and economic exergy in different components of the CCHP cycle were simulated by EES software. This software has a subset of various fluid properties that will be useful for simulating the use of different fluids in different parts of the simultaneous production of power, heat and cooling in a Kalina cycle. To simulate the combined cycle, the initial inputs in the base states is in accordance with Table 4.

Using the input items according to Table and the equations balance of mass and energy-related relationships, output values related to rate energy and exergy of various components of the cycle, also the effieciency of the exergy of the components are listed in Table 5.

Table 4. input parameter in simulation

Parameter	value
Reference Temperature, T_0	293 K
Reference Pressure, P_0	1 bar
Separator 1 Pressure, P_{sep1}	45 bar
Separator 2 Pressure, P_{sep2}	12 bar
Mass flow rate of solar collector	30 kg.s^{-1}
Pump isentropic efficiency, $\eta_{is,pum}$	85 %
Turbine isentropic efficiency, $\eta_{is,tur}$	85 %
Expander isentropic efficiency, $\eta_{is,expa}$	75 %
Compressor isentropic efficiency, $\eta_{is,comp}$	85 %
Evaporator temperature, T_{eva}	283 K
Condenser 2 temperature, T_{con2}	308 K
Heating unit temperature, T_{HU}	323 K
Ammonia mass fraction of basic solution, X_B	55 %
Condenser inlet temperature, $T_{24,26}$	298 K
Condenser outlet temperature, $T_{25,27}$	303 K

Table 5. Energy and exergy result for cchp cycle

Component	$\dot{Q}$ or $\dot{W}$(kW)	$\dot{I}_D$(kW)	η_{ex}(%)
Condenser 1	1956	63.78	44
Condenser 2	5126	319.9	29
Compressor	440.3	43.97	90
Evaporator	1611	57.23	46.8
Expander	489.7	141.5	77.6
Expansion valve	-	12.48	99.96
Heating Unit	1970	30.88	88.4
Mixer 1	-	6.29	100
Mixer 2	-	181	99.87
Mixer 3	-	1.327	100
Pump 1	25.77	2.64	89.8
Pump 2	46.79	7.586	83.8
Pump 3	0.4937	0.089	82
Separator 1	-	0	100
Separator 2	-	0.23	100
Separator 3	-	1.115	100
Turbine	276.5	42.73	86.6
Vapor generator	7700	315.7	83.8

Table 6. Energy and exergy result for collectors($G_{tot} = 1000\ W/m^2$)

Collector type	η_{col}(%)	$\dot{E}x_{col}$	$\dot{I}_D$	$\eta_{ex,col}$(%)
Vacuum tube	56.62	12715	10768	15.3
PTC	73.73	9765	7817	19.9
LFR	64.3	11195	9248	17.4
Dish	62.55	11508	9561	16.9

Table 7. Energy and exergy result for cchp cycle($G_{tot} = 1000\ W/m^2$)

Collector type	$\eta_{ex,cchp}$(%)	$\eta_{en,cchp}$(%)	$\dot{I}_{D,cchp}$
Vacuum tube	4.228	28.19	11996
PTC	5.506	36.71	9046
LFR	4.802	32.02	10476
Dish	4.672	31.15	10790

As seen, more exergy destruction is observed in collectors and then in the condenser 2. The high amount of exergy destruction in collectors is due to their high heat losses and high amount of exergy destruction in the condensers is due of fluid phase change in this heat exchangers. Also, the highest and lowest amount of exergy efficiency in the cycle belongs to the separators, mixers and condenser 2 respectively.

The overall exergy destruction for cchp cycle for each collector is mentioned in Table 6.

In Table 7, energy and exergy efficiency and exergy destruction are mentioned for CCHP cycle and four different collectors. Also, the amount of output work is 252.9W for the entire cycle.

Table 8. Exergeoeconomic result for cchp cycle

component	$\dot{Z}$(\$/yr)	$\dot{C}_D$(\$/yr)	r	f(%)
Vacuum tube	1634	164100	0	0.00986
PTC collector	1255	119134	0	0.01042
LFR collector	1439	140939	0	0.01011
Dish collector	1479	145711	0	0.1005
Turbine	47785	5077	0	0.904
Evaporator	6621	6805	1.441	0.4931
Expander	71301	16805	0	0.8093
Condenser 1	1538	7578	0.4609	0.1687
Condenser 2	2954	38000	0.5873	0.07214
Pump 1	239.1	313.6	0.00084	0.4326
Pump 2	279.2	909.8	0.00058	0.2348
Pump 3	85.52	10.58	0.00168	0.89
Heating unit	1669	3808	0.9411	0.3048
Compressor	33548	5224	0.03788	0.8653
Vapor generator	5581	42688	0.00883	0.1156
Separator 1	0	0.752	0	0
Separator 2	0	28.07	0	0
Separator 3	0	132.5	0	0
Mixer 1	0	1496	0	0
Mixer 2	0	65606	0	0
Mixer 3	0	317.1	0	0

The total value of exergeoeconomic factor for the cchp cycle and vacuum tube collector is 33%, 36% for PTC collector, 34.5% for LFR collector and for Dish collector, it is 34.2%. These values indicate that 64-67% of the system cost is the cost corresponding to the exergy destruction. As e result, using higher cost components that reduce the cost of exergy destruction and increase the initial cost of the system will improve the performance of the system from the perspective of economic exergy. Also, the total cost rate for the cchp cycle, for the vacuum tube collector is 533615 \$/yr, 488270 \$/yr for PTC collector, 510258 \$/yr for LFR collector and for Dish collector, it is 515071 \$/yr.

Also $\dot{C}_{W,net}$ or the net electricity cost rate of the ammonia-water mixture CCHP system 72350 \$.yr^{-1} was obtained.

7. Parametric study

The effects of some critical thermodynamic parameters (i.e., separator 1 pressure, condenser 2 temperature, evaporation temperature, heating unit temperature, and ammonia mass fraction) on the key performance criteria, including exergy efficiency, energy efficiency, cooling capacity, heating capacity and net output electricity are studied in this part. Also, the effect of radiation intensity, collector type and change the area of each collector on collector efficiency, exergy efficiency and cchp cycle exergy were investigated.

8.1. The effect of separator 1 pressure (P_{sep1}) on the system

The effect of separator 1 pressure on the energy efficiency, cooling capacity, exergy efficiency, heating capacity and net output electricity of the proposed CCHP system is sketched in Figures.2,3 and 4. As separator 1 pressure increases, turbines 1 and 2 output powers are decreased and increased, respectively. thus the overall turbines output electricity(turbine 1 plus expander output electricity) will be increased as separator 1 pressure increases. Moreover, the rich solution mass flow rate at separator 3 is decreased as separator 1 pressure increases. Furthermore, increasing separator 1 pressure will increase specific energy at the outlet of heating unit (HU) (state 14), while will decrease specific energy of the compressed solution (state 13). Hence, the enthalpy difference through the HU will decrease as separator 1 pressure increases. These two factors (decrease in the mass flow rate and enthalpy difference through the HU) will decrease the heating capacity as separator 1 pressure increases. Also, the cooling capacity reduces as separator 1 pressure increases.

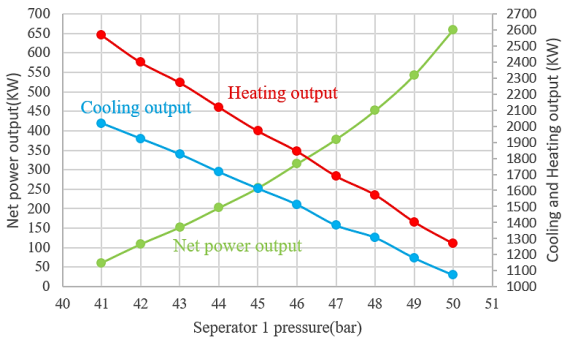

Figure 2. The effect of separator 1 pressure change on net power, Cooling and Heating output of the CCHP cycle

Fig. 3 also illustrates variation of the energy efficiencies for solar collectors versus various separator 1 pressures. Increasing separator 1 pressure decreases specific enthalpy of the heat source at the outlet of vapor generator, and hence more heat is required to be supplied to the system. Hence, the vapor generator duty will be increased. Through this study it is figured out that increasing rate of the net output electricity is considerably lower than the decreasing rate of the heating and cooling capacities plus augmentation rate of the vapor generator duty. Therefore, the energy efficiency will be decreased with the increase of separator 1 pressure.

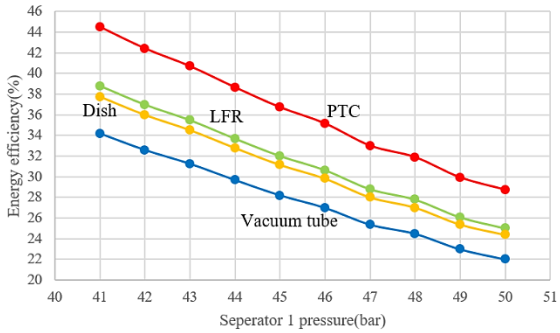

Figure 3. The effect of separator 1 pressure change on Energy efficiency of the CCHP cycle (for 4 collector types)

It is observed net output electricity is higher than the reduction rate of cooling and heating exergies. Hence, the exergy efficiency will be increased as separator 1 pressure increases.

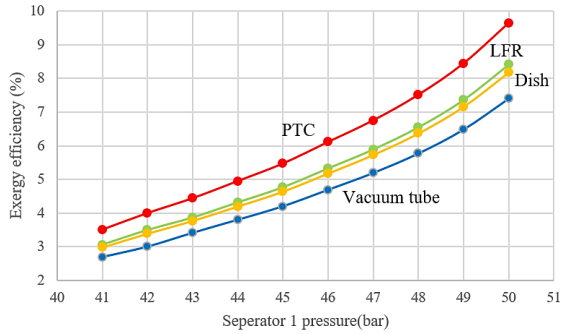

Figure 4. Change the exergy efficiency of the CCHP cycle with separator 1 pressure changes (for 4 collector types)

8.2. The effect of condenser 2 temperature (T_{con2}) on the system

Figures. 5,6 and 7 shows the effect of condenser 2 temperature on the energy efficiency, cooling capacity, exergy efficiency, heating capacity and net output electricity of the proposed cchp cycle. Increasing the condenser 2 temperature increases specific enthalpy at the outlet of expander (state 9), and hence expander output power will be decreased. increasing condenser 2 temperature decreases the consumed power of compressor since enthalpy difference through this component is decreased. However, that condenser 2 temperature has no considerable effect on the pumps consumed power along with turbine 1 output power. Therefore, net output electricity variation will depend on expander and compressor powers. Since reduction rate of compressor consumed power is higher than that of the expander output power, thus the net output electricity will increase as condenser 2 temperature increases. As Fig. 5 indicates, cooling and heating capacities are decreased with the increase of condenser 2 temperature, increase in the condenser 2 temperature decreases inlet enthalpy of heating unit, and hence the heating capacity will be decreased. Also, enthalpy value at the outlet of evaporator is decreased with the increase of condenser 2 temperature, thus the cooling capacity will be decreased, hence energy efficiency is reduced.

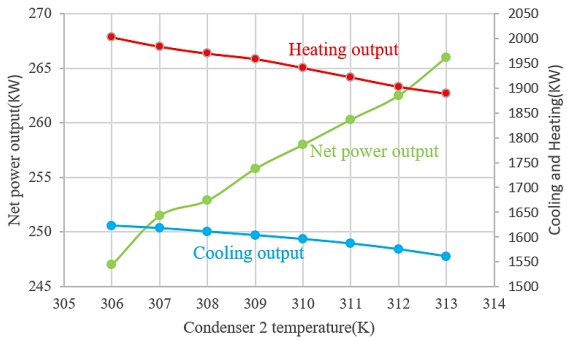

Figure 5. The effect of condenser 2 temperature change on net power, Cooling and Heating output of the CCHP cycle

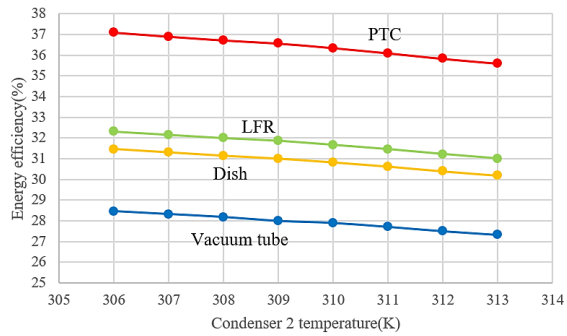

Figure 6. The effect of condenser 2 temperature change on Energy efficiency of the CCHP cycle (for 4 collector types)

The exergy efficiency of the system increases with increasing condenser 2 temperature. And main reason is the increase in net power output.

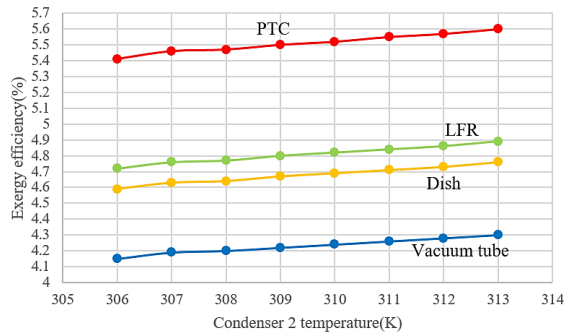

Figure 7. Change the exergy efficiency of the CCHP cycle with condenser 2 temperature changes (for 4 collector types)

8.3. The effect of evaporator temperature (T_{eva}) on the system

Figures. 8,9 and 10 has shown the effect of evaporation temperature on the cooling capacity, heating capacity, net output electricity, energy efficiency and exergy efficiency, respectively. increasing the evaporation temperature does not affect the turbines output power and pump 3 consumed power, while increases consumed power of compressor and pump 2 and increases pump 1 input power. However, the output power of pump 2 is increased with the increase of evaporation temperature since enthalpy difference through this component is increased so slightly. As a result of all these variations, the net output electricity of the system will be decreased as evaporation temperature increases. Moreover, as evaporation temperature increases, the heating and cooling capacities are increased ,Increasing evaporation temperature increases enthalpy difference through the heating unit, and hence the heating capacity will be increased. increasing evaporation temperature increases enthalpy at the outlet of this component, resulting in increase of cooling capacity. Therefore, the energy efficiency will be increased as evaporation temperature increases.

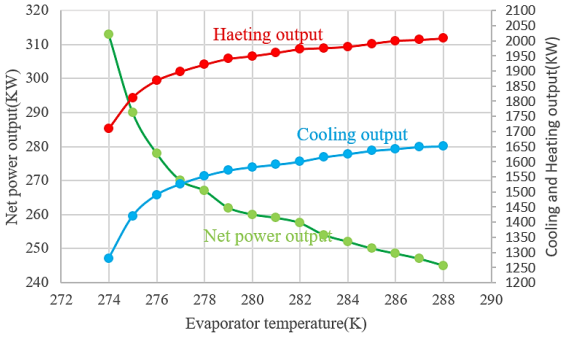

Figure 8. The effect of evaporator temperature change on net power, Cooling and Heating output of the CCHP cycle

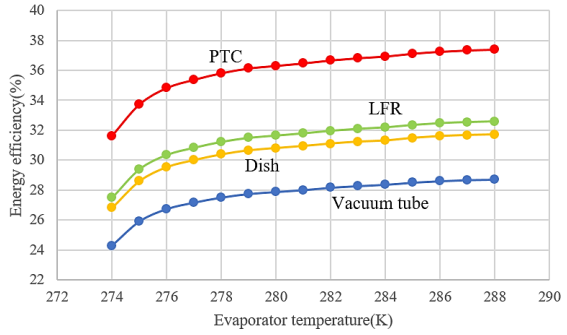

Figure 9. The effect of evaporator temperature change on Energy efficiency of the CCHP cycle (for 4 collector types)

Exergy efficiency decreases as evaporation temperature increases. As evaporation temperature increases, the exergy rates of heating and cooling are increased, but reduction rate of net output electricity is considerably higher than that the heating and cooling exergy rates.

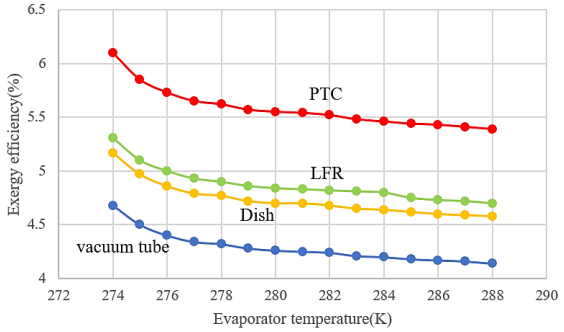

Figure 10. Change the exergy efficiency of the CCHP cycle with evaporator temperature changes (for 4 collector types)

8.4. The effect of ammonia concentration (X_B) on the system

Figures. 11,12 and 13 illustrates the effect of ammonia mass fraction on heating capacity, cooling capacity, energy efficiency, net output electricity and exergy efficiency, respectively. with increasing basic ammonia concentration will increase the turbines 1 and 2 output powers, Moreover, increasing basic ammonia concentration increases mass flow rate of ammonia solution through compressor, and hence the consumed power of compressor will be increased. Also, the mass flow rate of mixture through pumps 1 and 2 is decreased when basic ammonia concentration increases. and hence the consumed power of pumps 1 and 2 will be decreased and increasing basic ammonia concentration will raise mass flow rate of solution through pump 3 so slightly, and hence relatively more power is consumed by pump 3. thus the net output electricity of the system will be decreased when basic ammonia concentration increases.

The solution mass flow rate at separator 3 is increased as ammonia concentration increases, and hence the heating capacity will be increased and cooling capacity is raised when basic ammonia concentration increases. the reason that the mass flow rate of the solution through the separator 2 is increased when basic ammonia concentration increases.

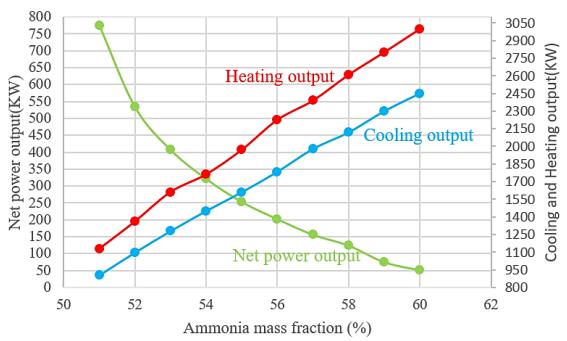

Figure 11. The effect of Ammonia mass fraction change on net power, Cooling and Heating output of the CCHP cycle

It is found that the decreasing rate of the net output electricity is lower than the rate of the heating and cooling capacities. Therefore, the energy efficiency will be increased with the increase of basic ammonia concentration.

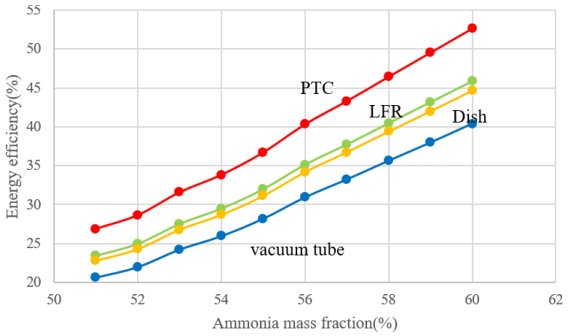

Figure 12. The effect of ammonia mass fraction change on Energy efficiency of the CCHP cycle (for 4 collector types)

It is observed that the decreasing rate of net output electricity is higher than the rate of increase cooling and heating exergies. Thus , exergy efficiency will be decreased.

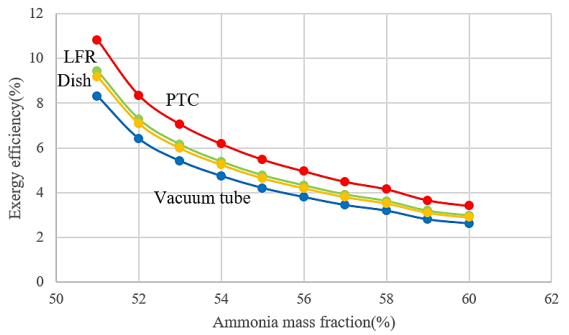

Figure 13. Change the exergy efficiency of the CCHP cycle with ammonia mass fraction changes (for 4 collector types)

8.5. The effect of heating unit temperature (T_{HU}) on the system

Figures. 14,15 and 16 are illustrated to show the effect of HU temperature on the heating capacity, cooling capacity and net output electricity, energy efficiency and exergy efficiency, respectively.

An increase in the HU temperature has no effect on turbines output power and pump 3 consumed power, while increases compressor and pump 1 consumed powers and decreases pump 2 input power. Thus, the net output power will be decreased as HU temperature increases. cooling capacity is remained constant with any variations in HU temperature, while heating capacity is increased with the increase of HU temperature. an increase in the HU temperature increases enthalpy difference through this component, and hence the heating capacity will be increased. and hence energy efficiency of the system will be decreased as HU temperature increases.

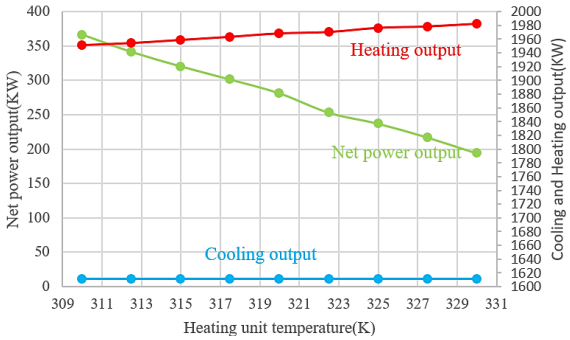

Figure 14. The effect of heating unit temperature change on net power, Cooling and Heating output of the CCHP cycle

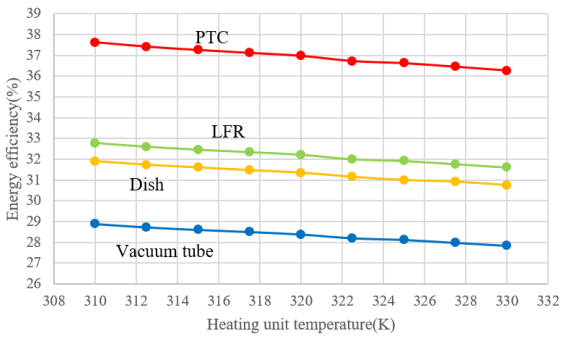

Figure 15. The effect of heating unit temperature change on Energy efficiency of the CCHP cycle (for 4 collector types)

However, reduction of net output electricity is considerably higher than the augmentation of heating and reduction of the supplied fuel exergy. As a result, the exergy efficiency of the cycle is decreased as HU temperature increases.

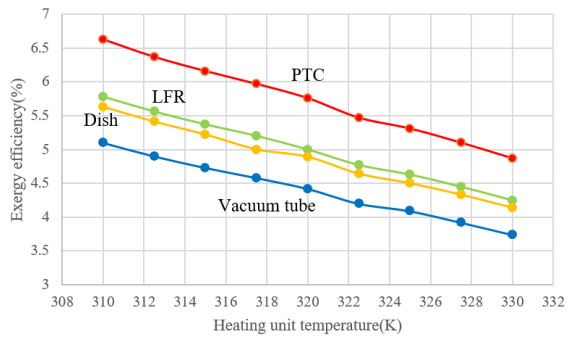

Figure 16. Change the exergy efficiency of the CCHP cycle with heating unit temperature changes (for 4 collector types)

8.6. The effect of intensity of the radiation (G_{tot}) and collector type on the system

Figures. 17 shows the effect of radiation intensity and collector type on collector area. In general, as the intensity of radiation increases, the area for primary energy supply

decreases. Due to the high efficiency of PTC collector compared to the other three collectors, the required area when using this collector is less. As can be seen in the figure, the effect of the collector type is very small as the radiation intensity increases. However, in low intensity radiation, there is a significant difference between the areas, which shows the importance of selecting the type of collector.

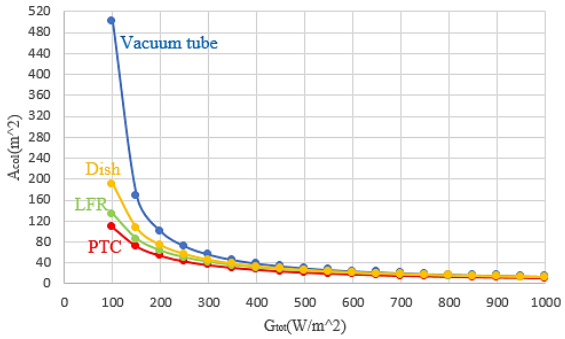

Figure 17. The effects of radiation intensity and collector type on collector area

Fig. 18 shows the effect of radiation intensity on collector efficiency. The effect of radiation intensity changes on the vacuum tube collector is greater then that of other three collectors. However, the PTC collector efficiency is higher than the othre three collectors.

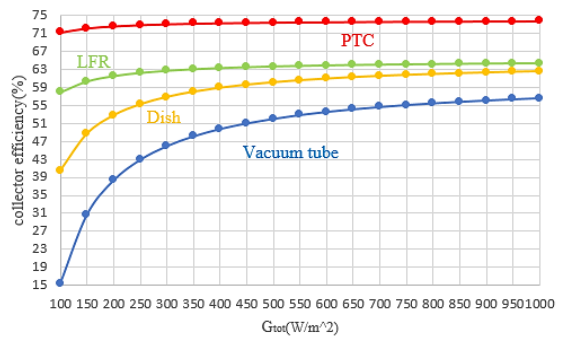

Figure 18. The effect of radiation intensity change on collector efficiency

Fig. 19 shows the effect of radiation intensity on the exergy efficiency of collectors, and because the exergy collectors are directly related to the radiation intensity and efficiency of collectors, in this case the PTC collector exergy efficiency is higher than the other three collectors.

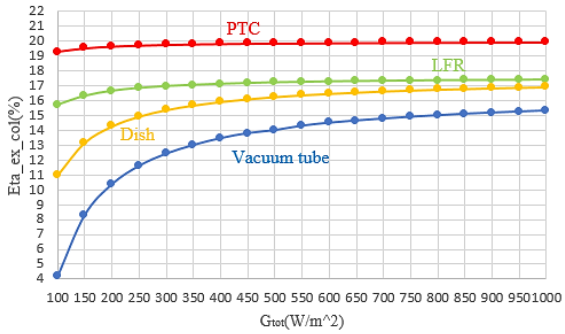

Figure 19. The effect of radiation intensity changes on the exergy efficiency of collectors.

Fig. 20 also shows the radiation changes on the total cycle exergy efficiency. As the radiation intensity increases due to the inrease in the exergy efficiency of each collector, the exergy efficiency of whole cycle also increases. Fig.21 also shows the energy efficiency of the whole cycle, it is clear that as the radiation on the collector surface increases, the energy efficiency of the whole cycle increases.

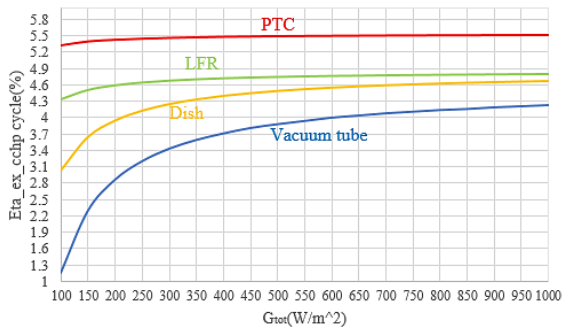

Figure 20. The effect of radiation intensity changes on the exergy efficiency of CCHP cycle.

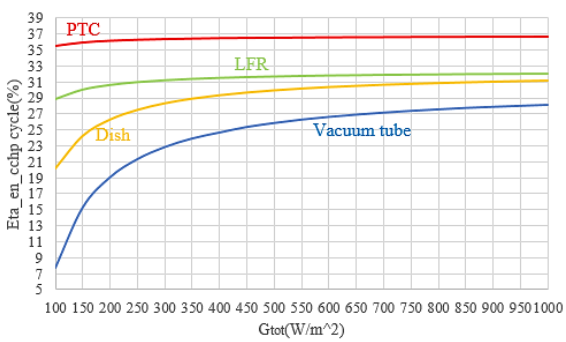

Figure 21. The effect of radiation intensity changes on energy efficiency of CCHP cycle

Figure.22 shows the effect of radiation intensity changes on the overall cost rate of the system. The effect of these changes on PTC collector is less than other collectors.

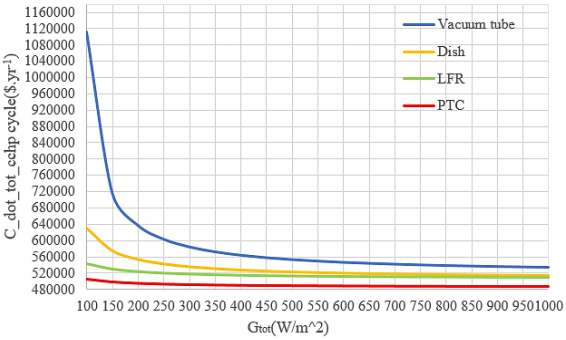

Figure 22. The effect of radiation intensity changes on the net cost rate of cchp cycle.

Figure. 23 also shows the effects of changes in radiation intensity on the overall exergy destruction of the cchp cycle. In this figure, the PTC collector has the least changes and vacuum tube collector has the most changes.

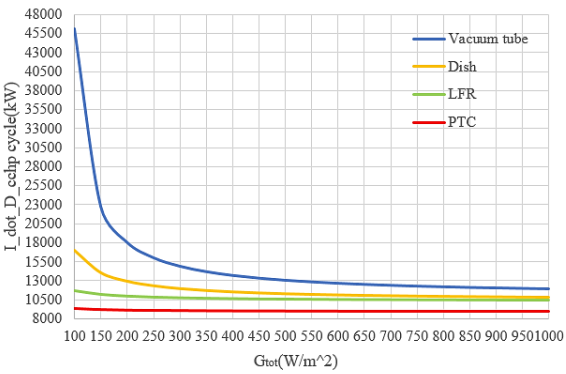

Figure 23. The effect of radiation intensity changes on the overall exergy destruction of cchp cycle.

8.7. The effect of collector area (A_{col}) and collector type on the system

Fig.24 shows the effect of vacuum tube collector area on energy and exergy efficiencies of total cycle. As the required area of the collector increases, the efficiency of the collector decreases and as a result, the energy and exergy efficiencies of entire cycle decreases.

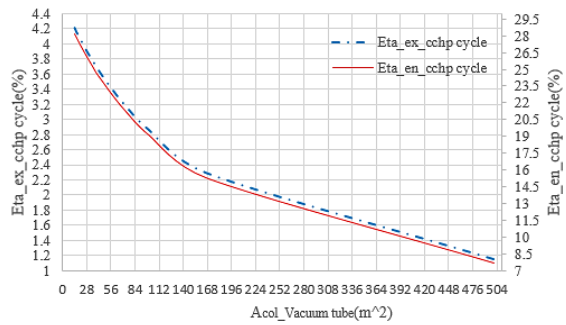

Figure 24. The effect of vacuum tube collector area changes on exergy and energy efficiencies of total cycle.

In the following figures(25 to 27), the changes in energy and exergy efficiencies of the cchp cycle are given in terms of changes in the area of the collector for three other collectors.

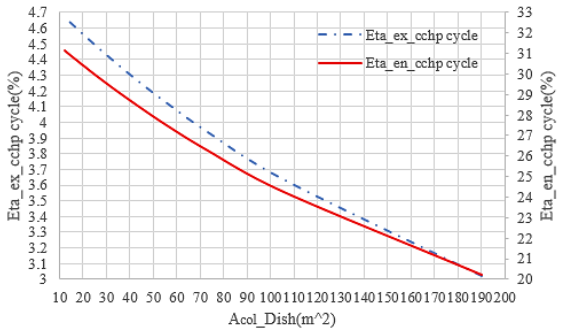

Figure 25. The effect of Dish collector area changes on exergy and energy efficiencies of total cycle.

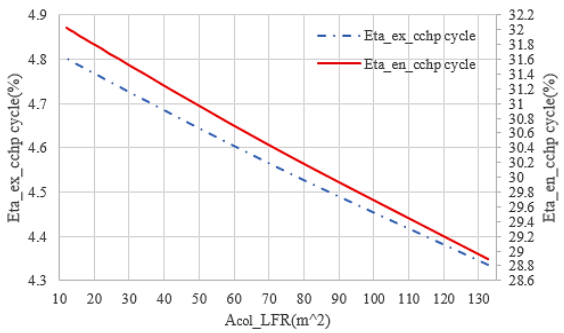

Figure 26. The effect of LFR collector area changes on exergy and energy efficiencies of total cycle.

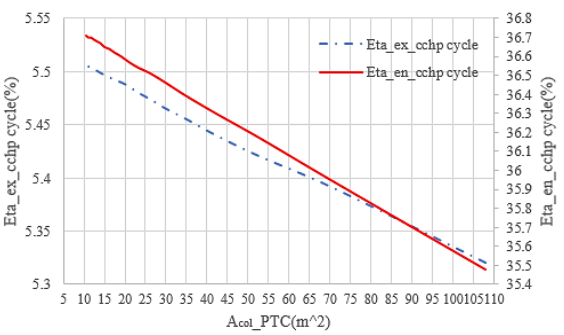

Figure 27. The effect of PTC collector area changes on exergy and energy efficiencies of total cycle.

9. Conclusions

An ammonia-water mixture CCHP system was analyzed from thermodynamics and exergeoeconomics perspectives. The analyzed system was based on kalina cycle and to provide the required heat in vapor generator, four types of vacuum tube, plate (Dish), linear share (LFR) and solar thermal linear (PTC) collectors were used. Some remark findings of the current investigation are as follows: Among all collectors, the PTC collector had the highest value of

exergy efficiency and lower value of exergy destruction. The analyzad trigeneration system could produce heating, cooling and net power output of 1611, 1970 and 252.9 kW, respectively. In this state with PTC collector, the energy efficiency, exergy efficiency and net cost rate of cchp cycle were calculated 36.71%, 5.506% and 488270 $/yr, respectively. Higher exergy and energy efficiencies may be obtained with increasing radiation intensity. But higher exergy efficiency may be achieved with increasing separator 1 pressure and condenser 2 temperature or with decreasing heating unit temperature. Also higher energy efficiency can be obtained with increasing evaporator temperature and ammonia mass fraction or with decreasing separator 1 pressure. The net cost rate of system with incresing radiation intensity can be decreased. It was found that the higher the radiation intensity received by the collector, the required area for the collector is reduced, thus, there is no difference between the collectors in the high radiation intensity. In general, the PTC collector has the highest efficiency compared to the LFR collector, Dish and then vacuum tube collector, and has the least area required to receive radaition intensity under same conditions.

Nomenclature

A	area (m^2)
c	cost per exergy unit ($/GJ^{-1})
$\dot{C}$	cost rate ($/yr^{-1})
CCHP	Combined cooling, heating and power
CRF	capital recovery factor
ex	exergy per unit mass (kW.kg^{-1})
f_k	exergeoeconomic factor
LMTD	Logarithmic mean temperature difference
LTHS	Low-temperature heat source
$\dot{m}$	mass flow rate (kg.s^{-1})
N	annual number of hours (hr)
r_k	Relative cost difference
U	overall heat transfer coefficient (kW.m^{-2}k^{-1})
C	further nomenclature continues down
X_B	Ammonia concentration
Z	investment cost of components ($)
$\dot{Z}$	investment cost rate of components ($.yr^{-1})
η	efficiency (%)
Φ_r	maintenance factor
ψ	exergy rate

References

1.Q. Chen, W. Han, J.-j. Zheng, J. Sui, and H.-g. Jin, "The exergy and energy level analysis of a combined cooling, heating and power system driven by a small scale gas turbine at off design condition," Applied Thermal Engineering, vol. 66, pp. 590-602, 2014.

2. Manolakos D, Kosmadakis G , Kyritsis S, Papadakis G On site experimental Evaluation of a low-temperature solar organic Rankine cycle system for RO desalination Solar Energy, 646–656, 2009

3. Wang X, Zhao L, Wang J, Zhang W, Zhao X, Wu W, "Performance evaluation of a low-temperature Rankine cycle system utilizing R٢٤٥fa", Solar Energy, 353–364, 2010.

4.[4]. M. Wang, Jiangfeng Wang, Yuzhu Zhao, Pan Zhao, Yiping Dai, "Thermodynamic analysis and Optimization of a solar-driven Regenerative organic Rankine cycle (ORC) based on flat-plate solar collectors", Applied Thermal Engineering, pp816-825, 2012.

5. J. Li, G. Pei, J. Ji, "Optimization of low temperature solar thermal electricgeneration with Organic RankineCycle in different areas, Appl", Energy, pp3355-3365, 2010.

6. X.D. Wang, L. Zhao, "Analysis of zeotropic mixtures used in low-temperature solar Rankine cycles for power generation, Sol", Energy, pp605-613, 2009.

7. Al-Sulaiman FA, Dincer I, Hamdullahpur F, "Thermoeconomic optimization of three trigeneration systems using organic Rankine cycles: Part I – Formulations", Energy Con Conversion and Management, pp199-208, 2013.

8. Al-Sulaiman FA, Hamdullahpur F, Dincer I, "Performance assessment of a novel system using parabolic trough solar collectors for combined cooling, heating, and power production", Renewable Energy, pp161-172, 2012.

9. Sotirios Karellas, Konstantinos Braimakis, "Energy–exergy analysis and economic investigation of a cogeneration and trigeneration ORC–VCC hybrid system utilizing biomass fuel and solar power", Energy Conversion and Management, pp103-113, 2006.

10.j.freeman, K Hellgardt ,c.n.markides ,assessment of solar powered organic rankine cycle systems for combined heating and power in uk domestic pplications, appliedenergy,vol .138,pp.605_20,2015.